Clays and Clay Minerals, Vol. 35, No. 3, 177–188, 1987.

CRYSTAL STRUCTURE OF A VERMICULITE-ANILINIUM INTERCALATE

P. G. SLADE,[1] C. DEAN,[2] P. K. SCHULTZ,[2] AND P. G. SELF[1]

[1] CSIRO, Division of Soils, Glen Osmond, South Australia 5064, Australia

[2] Physical and Inorganic Chemistry Department, University of Adelaide
Box 498 GPO, Adelaide 5001, Australia

Abstract—If anilinium ions are intercalated into Llano vermiculite, the stacking order of adjacent silicate layers is increased, resulting in a relatively sharp single crystal X-ray diffraction (XRD) pattern. The packing of intercalated organic members forms a superstructure and produces bonding from layer to layer which favors the stacking order. Superlattice reflections occur which, although sharp in the a^*b^* plane, are streaked along c^*. Apparently there is little coherence between adjacent layers of ordered organic units.

A three-dimensional set of XRD reflections for a triclinic sub-cell having the following lattice parameters was measured: $a = 5.326(3)$, $b = 9.264(4)$, $c = 14.82(5)$ Å, $\alpha = 90.31(7)$, $\beta = 96.70(6)$, and $\gamma = 89.55(5)°$. In this unit cell (symmetry $C1$), ditrigonal cavities in adjacent silicate layers are approximately opposite. Differential Fourier analyses and least-squares refinements showed that the principal axes of the anilinium ions, i.e., N–C(1)–C(4), are nearly perpendicular to the silicate layers. The planes of the aromatic rings, however, are about ±30° to X, neither parallel nor perpendicular to that direction, as indicated by earlier studies.

Inorganic cations and water molecules are also present in the interlayer; the former and some of the latter occupy sites near the middle of the layer. Anilinium-rich and anilinium-poor domains coexist. In the latter, the cation-water system predominates and apparently conforms to the superstructure. Although the cation-water structure could not be uniquely established from the reflections produced by the sub-cell, possible positional coordinates were obtained. From structural data for the silicate layers, no evidence was found for long-range Si/Al ordering in the tetrahedral sites.

Key Words—Anilinium ion, Crystal structure, Intercalate, Ordering, Vermiculite.

INTRODUCTION

The structures of intercalates formed between layer silicates and organic species are not readily determined by routine crystallographic methods. Such intercalates commonly lack three-dimensional periodicity because random faults may affect the mutual dispositions of the silicate layers and the intercalating organic molecules may not have regular configurations with respect to the layers. Further difficulties arise if superstructures are produced by the intercalation process. These superstructures produce sets of superlattice reflections which are not readily phased and, with the exception of a few, are weak; their information content therefore is limited.

Additional problems associated with the determination of intercalate structures arise if their organic components make only minor contributions to the total scattering from single crystals whose X-ray diffraction (XRD) patterns, at best, contain many weak reflections. Vermiculite-organic intercalates previously examined have yielded XRD patterns consisting of both sharp and diffuse $0kl$ reflections. Slade and Stone (1984) reported sharp $0kl$ reflections, indicative of a well-ordered structure, for anilinium-intercalated single crystals of vermiculite from Llano, Texas.

Previous work by Raupach *et al.* (1975), Slade *et al.* (1978), Slade and Raupach (1982), and Slade and Stone (1983) made use of superlattice reflections to characterize the well-ordered arrays formed when some organic species were intercalated into vermiculites. Particular note was taken that benzidine, 4-4′-diamino-*trans*-stilbene, and anilinium all gave rise to a single type of superlattice. Further unpublished work in this CSIRO Division has shown that a vermiculite-p-toluidine intercalate also gives similar XRD superlattice reflections.

The superlattice of all the intercalates listed above is manifest in their a^*b^* reciprocal lattice planes as a series of sharp, extra reflections which violate the C-face centering of the 5 × 9 Å unit cell of the parent vermiculite and indicate that the true cell has a dimension of 10 × 18 Å (i.e., $2a \times 2b$). The additional reflections, however, appear as diffuse rods in the direction of c^*, thus showing that little coherence exists between the relatively well-ordered arrays of organic species on individual layers. The organic molecules therefore are not on an ordered three-dimensional lattice through the whole crystal, and the superstructure is essentially two-dimensional.

Although some aspects of the interlayer structure of anilinium-vermiculite were established by Slade and Stone (1983, 1984) from one- and two-dimensional Fourier projections, a more comprehensive study has awaited the collection and analysis of the relatively

Copyright © 1987, The Clay Minerals Society

https://doi.org/10.1346/CCMN.1987.0350303 Published online by Cambridge University Press

Table 1. Unit-cell parameters of the Llano vermiculite-anilinium intercalate.

	From X-ray diffraction photographs	Used for this study[1]
a	5.29(5) Å	5.326
b	9.19(9) Å	9.264
c	14.76(15) Å	14.82
α	90.1(3)°	90.31
β	97.0(3)°	96.70
γ	89.5(2)°	89.55

[1] Crystal data based upon this unit cell are as follows: Unit-cell volume V = 726.02 Å^3, Z = 2, D_m = 2.21 g/cm^3, D_c = 2.30 g/cm^3, μ = 8.39 cm^{-1} (MoKα).

high-quality three-dimensional XRD data for this material. For the present study of the structure of anilinium-vermiculite the measurement of superlattice reflections was considered to be impractical because of their rod-like character. Accordingly the analysis was based upon three-dimensional data collected for a subcell of the superstructure.

EXPERIMENTAL

Determination of the unit-cell dimensions

XRD photographs reported by Slade and Stone (1983, 1984) of the zero layers about the a and b axes suggested that the unit cell of anilinium-vermiculite was monoclinic and that it contained only a single silicate layer having c = 14.89 Å. For the present study, upper-layer Weissenberg photographs about the a axis of a crystal of the material described by Slade and Stone (1983) were taken with CoKα radiation. The photograph for the second layer ($2kl$ reflections) not only showed b^* curving as expected for a monoclinic unit cell with a β angle of ~97°, but it also showed a small curvature in c^*; hence, the true unit cell is triclinic. A computer-simulated Weissenberg template for this reciprocal lattice layer showed that such a curvature results if the unit cell has a γ value of =89.5°. The unit-cell parameters deduced from Weissenberg and precession films are shown in column 1 of Table 1. On the basis of these values a SUPPER two-circle diffractometer was used to establish a more accurate set of unit-cell parameters. The results, given in column 2 of Table 1, describe the triclinic unit cell which was used as the basis for the subsequent intensity determinations.

Electron microprobe analyses

Electron microprobe analyses were carried out on the sodium-saturated and anilinium-intercalated vermiculites referred to by Slade and Stone (1983). Several crystals of each material were mounted on blank Araldite briquettes, coated with about 25 nm of carbon, and analyzed with a JEOL 733 Superprobe using a KEVEX 7000 series energy-dispersive system. The accelerating voltage was 15 kV; the beam current and diameter were 5 nA and 20 μm, respectively; and all counting times were 60 s. The results shown in Table 2 were obtained from the data after ZAF correction with PIBS software (Ware, 1981).

Table 2. Electron microprobe analysis of Llano vermiculite before and after anilinium intercalation.

	Before intercalation (Na-saturated) wt. %		After intercalation with anilinium ions wt. %		
SiO_2	37.4		37.2		
Al_2O_3	13.2		12.4		
Fe_2O_3	0.58		0.42		
TiO_2	0.21		0.26		
MgO	25.8		23.40		
Na_2O	6.25		not detectable		
Sum of oxides	83.44		73.68		
H_2O (difference)	16.56		[1]An_2O 12.80		
			13.52		
	Cations per 11 oxygens		Cations per 11 oxygens		Cations per 2.86 silicons
Si	2.86	4.00	3.01	4.00	2.86 3.99
Al^{IV}	1.14		0.99		1.13
Al^{VI}	0.05		0.20		
Fe^{2+}	0.03		0.03		0.03
Ti	0.01	3.03	0.02	3.06	0.02 2.73
Mg	2.94		2.82		2.68
Na	0.93	0.93	An 0.61		0.58
H_2O	4.23		H_2O 3.65		3.47

[1] Oxide equivalent of anilinium (An) calculated from the C and N analyses from the Australian Microanalytical Service.

Data collection

The crystal used was that on which the upper-layer Weissenberg photographs had been taken. It measured 900 × 530 × 20 μm. Three-dimensional intensity data were collected with a SUPPER two-circle diffractometer; its controlling algorithm incorporated the refinements previously discussed by Slade and Stone (1983). Equi-inclination geometry was used to record data from five reciprocal lattice layers along the [100] rotation axis. The index ranges were: $0 \leqq h \leqq 4$, $-10 \leqq k \leqq 10$, and $-20 \leqq l \leqq 20$. An $\omega/2\theta$ step-scan mode and filtered MoKα radiation were employed. To increase the reliability of the intensity measurements, especially for the weak reflections which comprised a very significant portion of the total diffraction pattern, counting was prolonged between 30 and 100 s at each 0.05° step of the scan range ($\Delta\omega$). $\Delta\omega$ was varied according to the formula of Guss *et al.* (1970). Of the 1928 unique reflections which were measured, 1825 were above zero intensity. Experimental intensities were corrected for Lp factors and absorption (linear absorption coefficient = 8.39 cm^{-1}). The transmission factors ranged between 0.95 and 0.70. The space group assumed for the data collection was $P1$, with the additional con-

https://doi.org/10.1346/CCMN.1987.0350303 Published online by Cambridge University Press

dition of C-face centering. Structure amplitudes were not squared before use in refinement.

Initial adjustment of silicate-layer parameters

To phase the structure amplitudes, a trial model for the silicate atoms was derived from the atomic coordinates given by Slade and Stone (1984). Because the present work showed the structure to be triclinic and because superlattice reflections were not included in the data set, the asymmetric unit chosen had the lowest symmetry likely to be shown by the silicate-only portion of the structure viz. C1. (The nonprimitive unit cell with C1 symmetry enables the structure to be directly compared with those of other layer silicates.) The interlayer structure as determined by X-rays represents an average over many cells, each of which is able to incorporate an organic molecule in one of four equivalent sites. Because the average structure was expected to have a center of symmetry, the origin of the cell used for this work was moved by $b/6$ with respect to the cell origin previously chosen by Slade and Stone (1984).

For the octahedral and tetrahedral cation sites, "mixed-atom" scattering factors were computed from the structural formula based on 2.86 silicons (Table 2), in conjunction with the scattering curves for fully ionized cations. For oxygen, two scattering curves were used—initially only that for non-ionized atoms was used, but as refinement proceeded the octahedral anions were found to be more appropriately assigned to the O^{2-} curve of Tokonami (1965). All other curves were taken from the International Tables for X-ray Crystallography (1974).

After the scaling factors for the reciprocal lattice layers were adjusted, the positional parameters for pseudo-symmetrically related atoms were adjusted independently. The position of one octahedral cation was fixed at 0,½,0 in all refinements. The isotropic temperature factors for pseudo-symmetrically related atoms were independently adjusted. For these initial calculations unit weights were used and reflections for which $|Fo|/<0.5$ and $\|Fo| - |Fc\| > 3.0$ were excluded. All positional parameters were then adjusted simultaneously in two cycles of refinement, followed by two more cycles during which all the temperature factors were released to given an R factor of 17.5% on 1685 reflections.

The peak profiles of all reflections with $\|Fo| - |Fc\| > 3$ were inspected for any obvious measurement errors. A significant number were found to be affected by overlap with adjacent peaks or counting problems. Where possible, peak profiles were re-determined and new structure amplitudes were calculated.

After these corrections were made, the three-dimensional difference Fourier maps described in the next section were computed. The maps represent the residual electron densities after subtraction of the electron densities described by the model for the silicate portion only. The interlayer atomic sites therefore show up as strong peaks.

Positioning of the anilinium ions from difference Fourier maps

The sections, shown in Figure 1, were sited according to the positions at which the organic interlayer atoms were expected from the previously published one- and two-dimensional projections. Figure 1a, the section at $y = ½$, shows substantial peaks in pairs on opposite sides of the interlayer. For comparison, two aniline molecules are shown drawn at the same scale. (Note that only the carbon atoms along the line between the upper and lower nitrogen atoms are close to the plane of this Fourier section.) Figure 1b is a section through the peak ascribed to nitrogen at $z = ⅔$ and Figures 1c and 1d are sections through the expected C(1) and C(4) positions. The peaks associated with these positions were well defined and helped to confirm that the principal axes of the anilinium groups, i.e., N–C(1) . . . C(4) are aligned approximately perpendicular to the silicate layers, as shown by Slade and Stone (1983, 1984).

The probable z coordinates for the carbon atoms C(2), C(3), C(5), and C(6), the "wing carbons," were determined from the known geometry of the aniline molecule (Brown, 1949). This known geometry also determined approximately where, on the appropriate Fourier sections, peaks belonging to the "wing carbons" might be. Figures 1e and 1f show the difference Fourier sections at $z = 0.46$ and $z = 0.55$ on which the "wing carbons" should be visible. Although other sections were computed, only those at $z = ½$, $x = ½$, $y = ⅙$, and $y = ⅚$ revealed significant extra interlayer peaks (Figure 2). The relative positions of the peaks shown in these sections indicated that cations and water molecules also occupied interlayer sites.

Initial refinement of parameters for interlayer organic atoms

Because four ditrigonal cavities are present in the unit cell under consideration four alternative ditrigonal rings of surface oxygen atoms exist to which the ammonium groups of the anilinium ions can be attached. Two rings surround the ditrigonal cavities in the silicate half-layer at the base of the cell, and two surround the cavities in the half-layer at the top of the cell. Due to the C-centering of the cell, however, only two of the ditrigonal rings are crystallographically unique.

For the postulated nitrogen sites a trial set of positional parameters was read from the Fourier maps and then refined by two cycles of least-squares. Subsequently, the trial site-occupancy factors assigned to each site (0.25) were varied during two additional cycles, and values of 0.23 and 0.31 for the lower and upper

https://doi.org/10.1346/CCMN.1987.0350303 Published online by Cambridge University Press

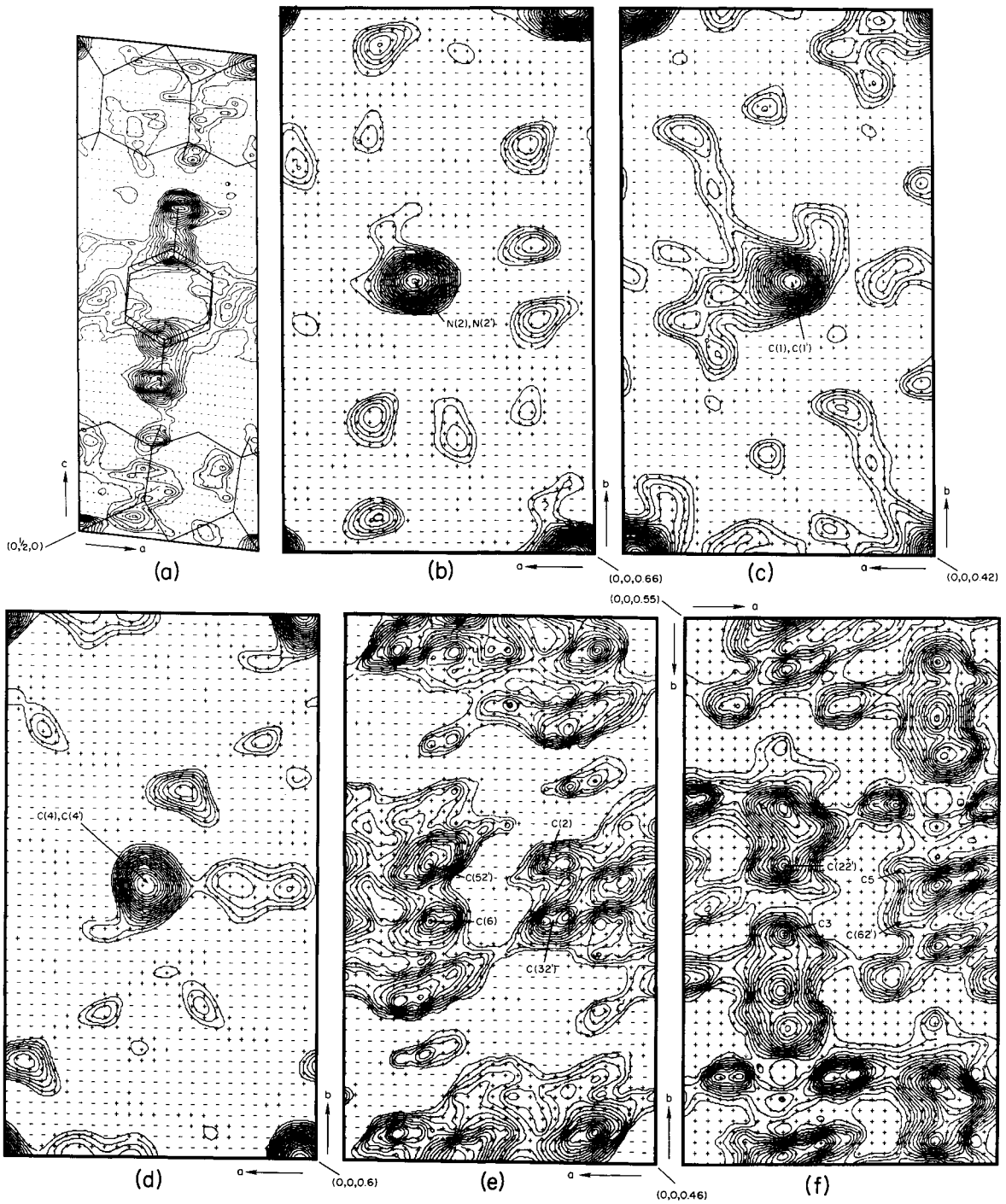

Figure 1. Difference Fourier (Fo − Fc) syntheses at (a) $y = ½$, (b) $z = ⅓$, (c) $z = 0.42$, (d) $z = 0.60$, (e) $z = 0.46$, and (f) $z = 0.55$. Contour interval used is 0.17 in (a) and 0.09 e/Å^3 in (b)–(f).

sites, respectively, were obtained. The temperature factors were arbitrarily maintained at B = 2.5. These adjustments reduced R by only 0.1%.

The relative insensitivity of the R factor to changes in the parameters for the interlayer atoms, compared with changes in parameters for silicate-layer atoms, prompted a transfer of the data and the partially adjusted model from the program ORFLS (Busing *et al.*, 1962) to the program SHELX (Sheldrick, 1976) for further calculations. The latter program allows a re-

https://doi.org/10.1346/CCMN.1987.0350303 Published online by Cambridge University Press

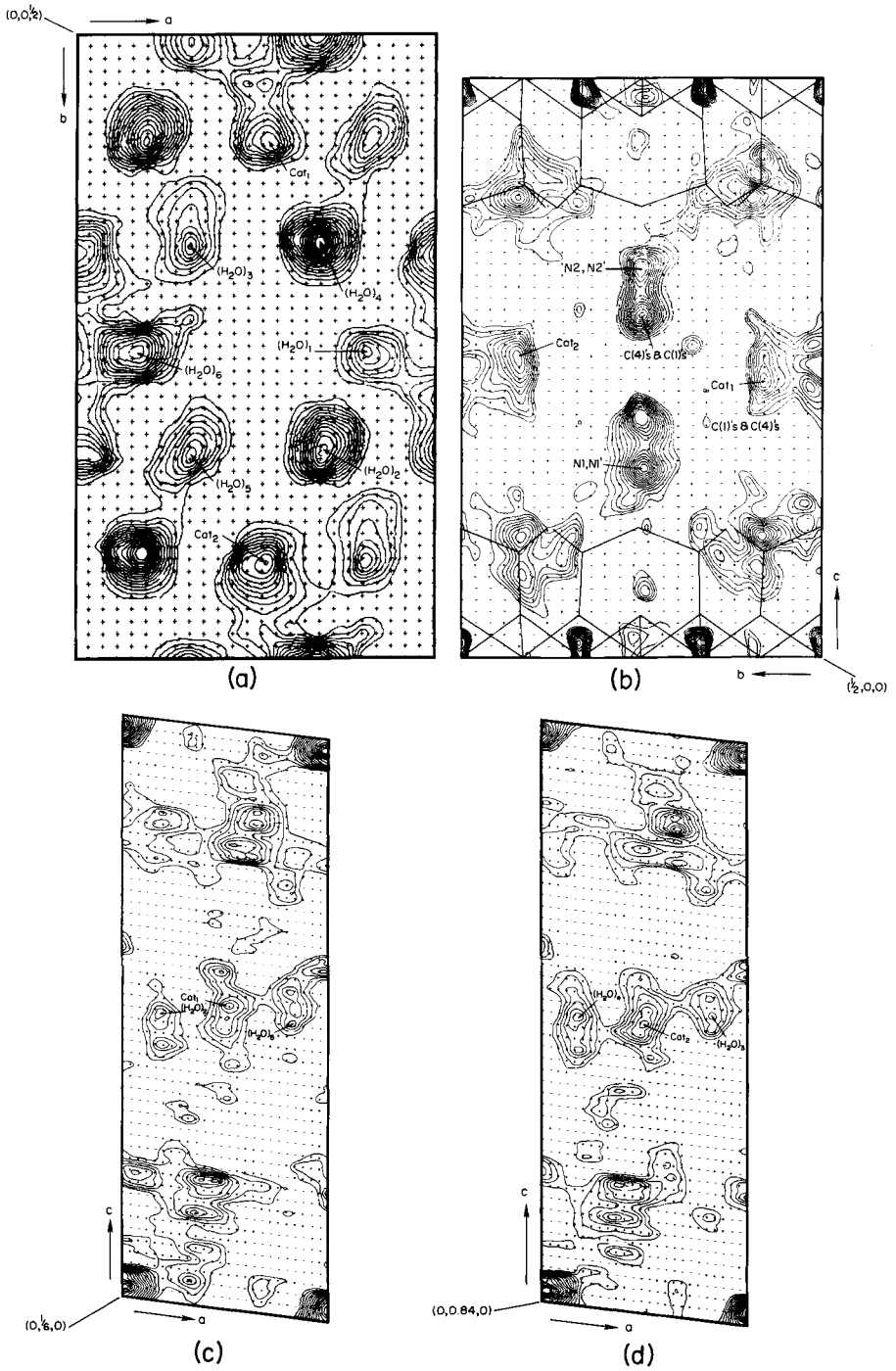

Figure 2. Three-dimensional (Fo − Fc) syntheses at (a) $z = ½$, (b) $x = ½$, (c) $y = ⅙$, and (d) $y = ⅚$. Contour intervals used are 0.09 e/Å^3 in (a) and (b) and 0.14 and 0.13 e/Å^3 in (c) and (d), respectively.

finement to be made of the parameters for a rigid group of atoms, and thereby produces a greater overall effect upon the least-squares fit. Furthermore, the program allows for the geometric idealization of positional parameters which, on input, may only approximate those of an aromatic ring. Aromatic hydrogens can also be placed in idealized positions. Of the 1928 measured reflections, 577 had $|F| < 0.7$ and were omitted from the structure refinement with SHELX which therefore used the remaining 1351 reflections.

https://doi.org/10.1346/CCMN.1987.0350303 Published online by Cambridge University Press

Table 3. Final positional and temperature parameters for the Llano vermiculite-anilinium intercalate.

Atom	*x*	*y*	*z*	B
Mg_1	0.0000	0.5000	0.0000	0.94(1)
Mg_2	−0.0030(1)	0.8309(1)	0.0013(6)	1.00(1)
Mg_3	−0.0012(7)	−0.8325(9)	0.0017(6)	0.75(1)
T_1	0.4079(6)	0.1597(8)	0.1832(6)	0.34(7)
T_2	0.4049(1)	0.8382(8)	0.1831(6)	0.59(1)
T_3	0.6176(9)	0.1713(9)	0.8141(6)	0.92(1)
T_4	0.6208(2)	0.8253(9)	0.8141(6)	1.15(1)
O_1	0.8604(7)	0.0012(6)	0.735(9)	1.01(2)
O_2	−0.8567(5)	0.0019(3)	−0.0673(8)	1.00(2)
O_3	0.3619(2)	0.1703(1)	0.0725(9)	0.87(2)
O_4	0.3584(1)	−0.1639(2)	0.0757(4)	0.87(2)
O_5	−0.3606(3)	0.1700(2)	−0.0704(1)	1.60(2)
O_6	−0.3521(2)	−0.1630(1)	−0.0743(5)	1.78(2)
O_7	0.1688(5)	0.2416(3)	0.2240(2)	2.48(2)
O_8	0.1787(5)	−0.2381(1)	0.2237(1)	1.65(2)
O_9	−0.1193(6)	0.2350(2)	−0.2252(6)	1.50(2)
O_{10}	−0.1236(5)	−0.2340(5)	−0.2244(8)	1.05(2)
O_{11}	0.4525(1)	0.0053(4)	0.2256(9)	1.14(2)
O_{12}	−0.4196(9)	0.0058(7)	−0.2239(7)	1.48(2)
N(1)	0.425(1)	0.487(5)	0.320(6)	2.2(2)
C(1)	0.443(4)	0.487(3)	0.410(3)	2.2(2)
C(2)	0.236(4)	0.528(3)	0.454(3)	2.2(2)
C(3)	0.255(4)	0.529(3)	0.548(3)	2.2(2)
C(4)	0.482(4)	0.488(3)	0.599(3)	2.2(2)
C(5)	0.589(4)	0.447(3)	0.555(3)	2.2(2)
C(6)	0.669(4)	0.446(3)	0.460(3)	2.2(2)
N(2)	0.565(6)	0.483(2)	0.667(4)	2.2(2)
C(12)	0.543(4)	0.466(3)	0.578(3)	2.2(2)
C(22)	0.350(4)	0.536(3)	0.523(3)	2.2(2)
C(32)	0.328(4)	0.517(3)	0.429(3)	2.2(2)
C(42)	0.499(4)	0.428(3)	0.390(3)	2.2(2)
C(52)	0.692(4)	0.358(3)	0.446(3)	2.2(2)
C(62)	0.714(4)	0.377(3)	0.540(3)	2.2(2)
N(1′)	0.459(1)	0.483(6)	0.310(3)	2.2(2)
C(1′)	0.529(4)	0.461(3)	0.397(3)	2.2(2)
C(2′)	0.371(4)	0.388(3)	0.450(3)	2.2(2)
C(3′)	0.448(4)	0.364(3)	0.542(3)	2.2(2)
C(4′)	0.682(4)	0.414(3)	0.582(3)	2.2(2)
C(5′)	0.840(4)	0.487(3)	0.529(3)	2.2(2)
C(6′)	0.764(4)	0.510(3)	0.437(3)	2.2(2)
N(2′)	0.575(2)	0.495(6)	0.676(7)	2.2(2)
C(12′)	0.538(4)	0.500(3)	0.586(3)	2.2(2)
C(22′)	0.319(4)	0.444(3)	0.539(3)	2.2(2)
C(32′)	0.284(4)	0.450(3)	0.444(3)	2.2(2)
C(42′)	0.467(4)	0.513(3)	0.397(3)	2.2(2)
C(52′)	0.686(4)	0.569(3)	0.445(3)	2.2(2)
C(62′)	0.722(4)	0.563(3)	0.539(3)	2.2(2)
Cat_1	0.5279(1)	0.1614(6)	0.4671(7)	5.5(4)
Cat_2	0.5116(8)	0.8424(7)	0.4978(2)	5.5(4)
$(H_2O)_1$	0.3217(7)	−0.0036(1)	0.4848(9)	5.0(4)
$(H_2O)_2$	0.2599(3)	0.1672(7)	0.4455(1)	5.0(4)
$(H_2O)_3$	0.2953(4)	0.3092(6)	0.4916(4)	5.0(4)
$(H_2O)_4$	0.7499(1)	0.2981(5)	0.4503(2)	5.0(4)
$(H_2O)_5$	0.8342(4)	0.1560(6)	0.4974(1)	5.0(4)
$(H_2O)_6$	0.5588(6)	0.0325(6)	0.4721(9)	5.0(4)

The tabulated observed and calculated structure factors and hydrogen atomic parameters are available on request from the first author.

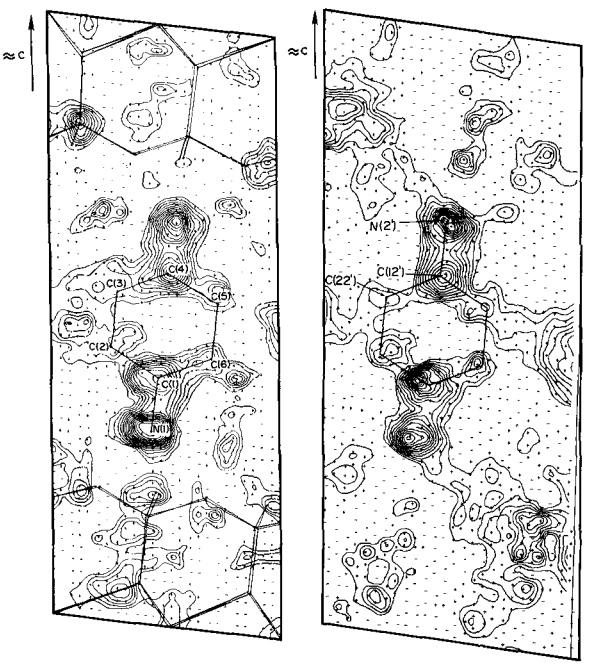

Figure 3. (left) Three-dimensional (Fo − Fc) syntheses in the planes defined by the coordinates of N(1), C(1), and C(2); and (right) by N(2′), C(12′), and C(22′). Contour intervals are 0.14 and 0.16 e/Å^3, respectively.

The chemical analysis indicated that an average unit cell contains 1.22 anilinium groups. If the probability of an anilinium ion being attached to the oxygens about one ditrigonal cavity is the same as the probability of its being attached to those about another cavity, the four sites will each have site occupancy factors of ~0.25. The average (0.27) of the experimentally determined site-occupancy factors for the nitrogen atoms is therefore close to the expected value.

The peaks ascribed to the "wing carbons" on the difference Fourier sections shown in Figures 1e and 1f indicated that individual organic cations had the planes of their aromatic rings directed at about ±30° to the *a*-axis of the unit cell. Because the "wing carbons" are not on the central axes of the molecules, these atoms have lower site-occupancy factors (0.13).

After obtaining a set of trial positional coordinates for the carbon atoms, the structure analysis was continued as follows. Initially SHELX was used to modify the coordinates to suit the geometry of the hexagonal aromatic-ring portion of an anilinium ion. The rigid group refinement option was then used to obtain the best positional coordinates for atoms in the four unique configurations adopted by the organic ions.

Fourier sections in the planes of the organic molecules

To obtain a satisfactory visual representation of the organic molecules, a program was written to project

https://doi.org/10.1346/CCMN.1987.0350303 Published online by Cambridge University Press

Table 4. Bond lengths for a selection of interlayer atoms and surface oxygen atoms.

Atoms	Distance (Å)
O_7–N(1)	2.93
O_8–N(1)	2.93
O_{11}–N(1)	2.74
O_9–N(2)	3.04
O_{10}–N(2)	2.84
O_{12}–N(2)	3.03
O_7–N(1′)	2.93
O_8–N(1′)	2.74
O_{11}–N(1′)	2.85
O_9–N(2′)	2.90
O_{10}–N(2′)	2.87
O_{12}–N(2′)	2.92
O_9–C(4)	3.55
O_{10}–C(4)	3.44
O_{12}–C(4)	3.58
O_7–C(42)	3.34
O_8–C(42)	3.14
O_{11}–C(42)	3.64
O_9–C(4′)	3.38
O_{10}–C(4′)	3.74
O_{12}–C(4′)	3.48
O_7–C(42′)	3.60
O_8–C(42′)	3.66
O_{11}–C(42′)	3.51

Standard deviation for all bond lengths is 0.03 Å.

the difference electron densities calculated by SHELX onto planes at any orientation in a unit cell and to contour the resultant maps. Each plane was specified by the coordinates of three atoms. Figures 3 (left) and 3 (right) show the difference electron densities on planes, each of which is defined by three atoms (one nitrogen and two carbon atoms), whose positions were established by the rigid group refinement.

Non-organic interlayer sites

As mentioned above, certain difference sections (e.g., at $x = ½$, $y = ½$, and $z = ½$) show peaks attributable to partially occupied interlayer cation and water sites. From the section at $x = ½$, Figure 2b, the cation sites arrowed at ($y = ⅙$ and $y = ⅚$, $z = ½$) show considerable positional variation and low levels of occupancy. The adjacent water sites seen in the other two sections, Figures 1a and 2a, are also diffuse and indicate that the water molecules may have different arrangements throughout the structure.

The principal arrangement adopted is apparent from the section at $z = ½$ (Figure 2a), which shows three weak and three stronger peaks about each cation site. To maintain water-water contact distances of about 2.8 Å, however, only three of the six sites about any one cation can be occupied. The alternative set of three sites can only be occupied in other cells. Apparently the water molecules form triangular clusters, the planes of which are tilted out of the plane at $z = ½$; the sections at $y = ½$ (Figure 1a) and $y = ⅙$ and $y = 0.84$ (Figures 2c and 2d) show the water peaks tail away from the plane at $z = ½$. In addition to the relatively well-developed peaks considered above, weaker ones exist at the positions occupied by water in two water-layer hydrates (Slade *et al.*, 1985).

The positional parameters and site occupancy factors for the interlayer cations (assigned to the scattering curve for Mg^{2+}) and the oxygens of the water molecules were refined by initially holding their thermal parameters fixed at 5.0 and 2.5, respectively. All parameters for the whole structure were then released, but for interlayer atoms of a similar kind group isotropic temperature factors and site occupancy factors were adjusted. The final R was 14.4% and R_w was 15.8% (Table 3). The weighting scheme applied gave reflections weights = $k/(1 + |g|F^2)$, where k and g were refined.

The presence of interlayer inorganic cations was unexpected inasmuch as none of the sodium which had saturated the exchange sites prior to the anilinium intercalation was found by a flame-photometric analysis of the intercalate itself. The identity of the residual, inorganic, interlayer cations is uncertain, but they are probably magnesium ions. These, along with aluminum ions, are released from vermiculite when it takes up anilinium ions from aqueous hydrochloride solutions at a pH of 2.8 (Dino Pisaniello, South Australian Health Commission, Adelaide, South Australia 5001, Australia, personal communication). A back-reaction was then responsible for the incorporation of the cations into the interlayer sites identified from the Fourier maps.

Residual silicate disorder

Although the intercalation of anilinium ions into Llano vermiculite orders the stacking of the silicate layers such that they have relative positions resembling those found in 1*M* mica-type structures, the process is not fully achieved throughout the crystal. Residual disorder is therefore present and is seen, for example, on the difference section at $z = 0.16$ (the level of the tetrahederal cations) where the positions at the centers of the rings of tetrahedra were found to be slightly occupied. Sections through the surface oxygens, parallel to the basal plane, also showed peaks associated with the residual disorder, but no extra peaks were found on a section through the octahedral cations. The residual disorder proved to be difficult to model, but it appeared to be largely associated with irregular shifts of the whole silicate layer by $\pm b/3$. Because the octahedral cations are already separated by $b/3$, no extra peaks on the section were present through the octahedral cations. Refinement of the site occupancy of the atoms as a group in the alternate $\pm b/3$ shifts showed

https://doi.org/10.1346/CCMN.1987.0350303 Published online by Cambridge University Press

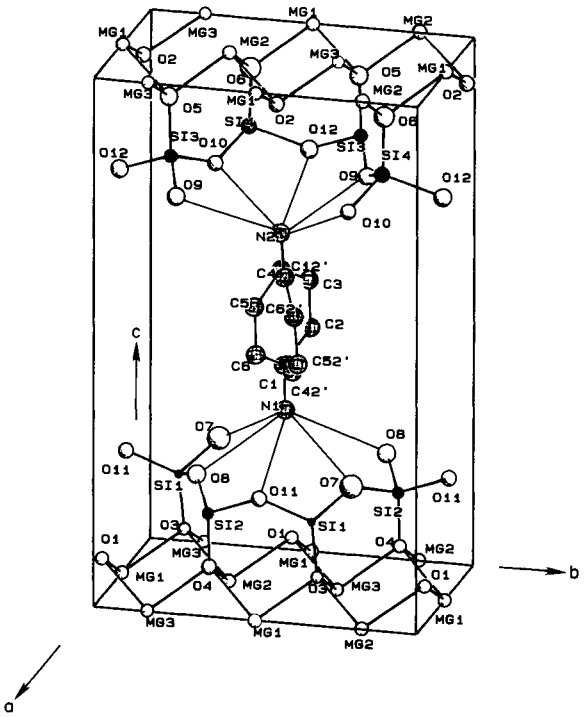

Figure 4. Structure of anilinium-intercalated Llano vermiculite. For clarity, only two of the four possible anilinium ions are shown.

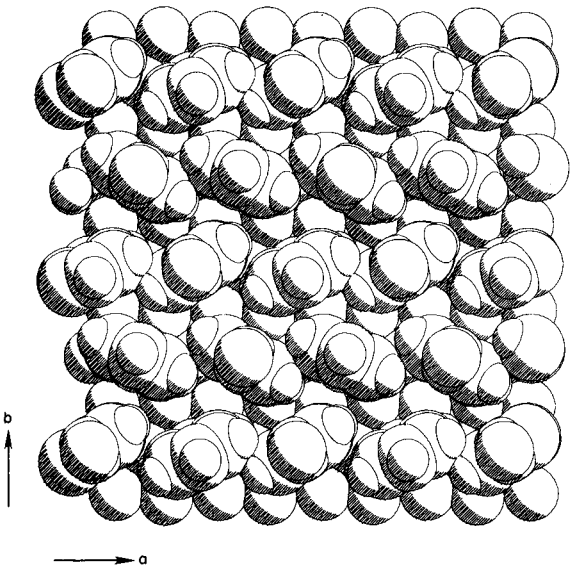

Figure 5. Computer drawing (PLUTO78) of anilinium ions in a closest packed domain in the interlayer region of the intercalate formed with Llano vermiculite. Anilinium ions, drawn to the same scale as the silicate surface oxygens, are shown with their amino groups directed alternately up and down. This arrangement is only one of the possible arrangements for these groups.

that the amount of each layer in a $+b/3$ or $-b/3$ position was ~5% of the total number of layers.

DISCUSSION

This study of anilinium-vermiculite illustrates some of the problems that can affect crystallographic work on clay-organic materials. For example, although anilinium ions and some substituted anilinium ions improve the stacking order in vermiculites, some degree of residual disorder remains. Part of the remainder probably results from an incomplete reaction between the organic species and the clay. Transmission electron micrographs of edge-on views of flakes of anilinium-intercalated and Mg-saturated Llano vermiculite showed randomly distributed packets of unopened (mica-like) layers.

Atoms having low site-occupancy factors can be difficult to locate. In this study "wing carbons," having site occupancy factors of only 0.13, were difficult to find. Fortunately, the higher occupancy factors for atoms along the axes of the aniline molecules enabled the ipso, C(1), and the para, C(4), carbons to be readily found. The true unit cell of the intercalate has four times the volume of the cell actually used in this study; therefore, the images of the interlayer structure, shown by the Fourier maps, are averages of the contents of the four different cells that together comprise the supercell. Although this averaging was confusing, the geometrical relationships possible between the organic atoms enabled the weak images of the "wing carbons" to be found. These atoms were more readily located because of the close proximity of the sites of carbon atoms in the upper and lower rings. Therefore, peaks belonging to the "wing carbons" were mutually reinforcing.

Although the earlier studies of Slade and Stone (1983, 1984), based only upon one- and two-dimensional Fourier projections, correctly located the nitrogen atoms and also the ipso and para carbons, the "wing carbons" were incorrectly located. As a result, the planes containing the aromatic rings were reported to be parallel and perpendicular to [010]. The present study, based upon three-dimensional data, has located the ring planes to be about $\pm 60°$ to [010]. In the vermiculite-anilinium intercalate (Figure 4) the planes of the aromatic rings are therefore similarly oriented to those proposed by Slade and Raupach (1982) for a vermiculite-benzidine intercalate.

Superstructure

A more serious difficulty associated with the description of the structure for the vermiculite-anilinium intercalate in a sub-cell, arises because the absolute positions of the inorganic cations, the water molecules, and the organic cations cannot readily be uniquely determined. To investigate how the superstructure might

https://doi.org/10.1346/CCMN.1987.0350303 Published online by Cambridge University Press

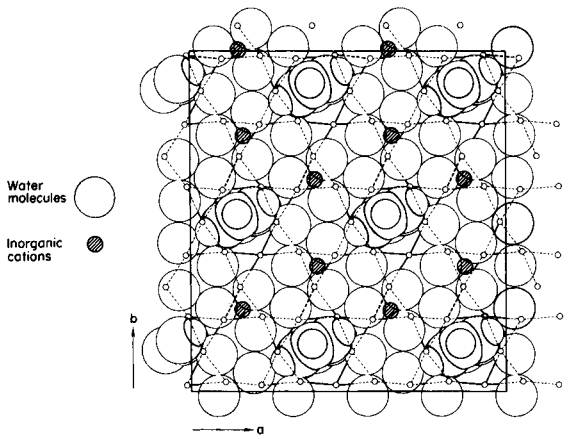

Figure 6. Computer drawing (PLUTO78) of water molecules, anilinium ions, and inorganic cations as might be organized in a domain having a low density of organic units. Overall the arrangement conforms to the superstructure.

govern the arrangement of water molecules and cations (both organic and inorganic), several possible arrangements were examined with the molecule drawing program PLUTO78 (Motherwell, 1978). For an average sub-cell to contain about one anilinium ion, each sub-cell must contain one organic unit. Alternatively, coexisting anilinium-rich and anilinium-poor domains might coexist throughout the crystal. No superstructure arrangement could be found in which each sub-cell contained an anilinium ion and also allowed for triangular groups of water molecules about cations positioned, as found, between tetrahedral bases. The alternative model, involving domains, was therefore examined.

Sub-cells in anilinium-rich domains can contain a maximum of two anilinium ions arranged as in Figure 5. A similar close-packed arrangement exists in aniline hydrochloride (Brown, 1949) and in aniline hydrobromide (Nitta *et al.,* 1948) and has been postulated for benzidine in a vermiculite-benzidine intercalate (Slade and Raupach, 1982). For the arrangement shown in Figure 5, the repeat distance along a row perpendicular to the *b*-axis is ~5.33 Å. This distance is also the intermolecular distance and the *b*-axis length in aniline hydrochloride. In aniline hydrobromide the anilinium groups are displaced alternately up and down in the direction of their N–C(1) . . . C(4) axes. The similar packing arrangement in the intercalated vermiculite maintains the interlayer separation.

To accommodate the triangular groups of water molecules expected about the inorganic cations, anilinium-poor domains must exist in the close-packed array shown in Figure 5. Figure 6, therefore, shows how water molecules can form triangular groups about cations in an anilinium-poor domain. The presence of such domains requires that anilinium ions must also exist in close-packed arrays so that the overall arrangement will consist alternately of more and less densely populated domains. In the overall domain system the arrangement of organic ions, water molecules, and metal cations must conform to the superstructure even while the intercalation reaction proceeds, because only one set of superlattice reflections has ever been observed.

Unpublished work carried out by the authors has shown that some vermiculites, for example, those from Young River, Western Australia, or Phalaborwa, Transvaal, can take up more anilinium ions than the material from Llano, Texas. The overall packing density can be expected to reflect the extent of organic uptake. In turn, the organic uptake will be governed by the layer charge and the competition between anilinium ions and those ions, initially from the clay, entering the interlayer via a back-reaction.

For large organic molecules to enter interlayer sites, both water molecules and cations must be removed. Thus, although the high layer charge of Llano vermiculite could have been expected to produce a complete coverage of the silicate layer surfaces by anilinium ions, the back reaction in the acidic medium used for the exchange restricted the coverage to about one half.

Elemental analyses

A comparison between the two lower left-hand columns of Table 2 shows an unlikely increase in the numbers of Si atoms in tetrahedral sites and an unlikely redistribution of Al between the silicate tetrahedral and octahedral sites. These results demonstrate that the formula is incorrectly calculated from the usual base of 11 oxygens.

The difficulty was overcome by assuming that the number of silicons in tetrahedral sites remained essentially constant during intercalation. The cation numbers for a formula unit were then recalculated from the constant silicon concentration. The lower right-hand column of Table 2 gives the intercalate's composition with respect to 2.86 silicons, the number in the original Na-vermiculite. The analytical data presented in this way suggest that cations were lost mainly from octahedral sites.

The octahedral cation deficiency, in association with the *elemental* analyses for the cationic components means that insufficient oxygen is accounted for when the elemental concentrations are converted to oxides. If these oxide sums plus the anilinium components are used to obtain the water content by difference, the results are too high, as can be seen from the values in the lower two right-hand columns of Table 2. These total water contents each include a single molecule of structural water per formula unit, but the number of water molecules remaining (2.65 per formula unit, or 5.3 per cell) still exceeds the number likely to be present in the interlayer region of an average unit cell. A re-

https://doi.org/10.1346/CCMN.1987.0350303 Published online by Cambridge University Press

Table 5. Interatomic distances and angles for the silicate layer atoms.

Tetrahedron about T(1)			
T(1)–O_3*	1.63 Å	O_3–O_7	2.66 Å
–O_7	1.65	–O_8	2.78
–O_8	1.78	O_7–O_8	2.73
–O_{11}	1.57	O_{11}–O_3	2.74
mean	1.66	–O_7	2.65
		mean	2.70
Tetrahedron about T(2)			
T(2)–O_4*	1.58 Å	O_4–O_7	2.74 Å
–O_7	1.71	–O_{11}	2.71
–O_8	1.58	O_8–O_4	2.59
–O_{11}	1.68	–O_7	2.62
mean	1.64	–O_{11}	2.69
		O_{11}–O_7	2.69
		mean	2.67
Tetrahedron about T(3)			
T(3)–O_5*	1.70 Å	O_9–O_5	2.83 Å
–O_9	1.69	O_{10}–O_5	2.69
–O_{10}	1.60	–O_9	2.70
–O_{12}	1.64	–O_{12}	2.64
mean	1.66	O_{12}–O_5	2.72
		–O_9	2.67
		mean	2.71
Tetrahedron about T(4)			
T(4)–O_6*	1.65 Å	O_6–O_{12}	2.71 Å
–O_9	1.59	O_9–O_6	2.68
–O_{10}	1.63	–O_{10}	2.66
–O_{12}	1.77	–O_{12}	2.73
mean	1.66	O_{10}–O_6	2.73
		–O_{12}	2.71
		mean	2.71
Octahedron about Mg_1			
Mg_1–OH(1)	2.09 Å	O_3–O_4	3.10 Å
–O_3	2.08	–OH(1)	3.07
–O_4	2.09	O_4–OH(1)	3.09
–OH(2)	2.04	O_5–O_6	3.09
–O_5	2.08	–OH(2)	3.08
–O_6	2.07	O_6–OH(2)	3.09
mean	2.08	mean (unshared)	3.09
		Shared edges between Mg_1 and Mg_3	
		O_3–OH(2)	2.74
		O_5–OH(1)	2.79
		O_6–O_4	2.85
		mean	2.79
Octahedron and Mg_2			
Mg_2–OH(1)	2.08 Å	O_3–O_4	3.06 Å
–O_3	2.01	–OH(1)	3.06
–O_4	2.10	O_4–OH(1)	3.05
–OH(2)	2.09	O_5–O_6	3.02
–O_5	2.02	–OH(2)	3.07
–O_6	2.08	O_6–OH(2)	3.05
mean	2.06	mean (unshared)	3.05
Shared edges between Mg_2 and Mg_3		Shared edges between Mg_1 and Mg_2	
OH(1)–OH(2)	2.71	O_3–O_5	2.72
O_3–O_6	2.80	O_4–OH(2)	2.76
O_4–O_5	2.80	O_6–OH(1)	2.80
mean	2.77	mean	2.76

https://doi.org/10.1346/CCMN.1987.0350303 Published online by Cambridge University Press

Table 5. Continued.

Octahedron about Mg_3			
Mg_3–OH(1)	2.07 Å	O_3–O_4	3.09
–O_3	2.09	–OH(1)	3.11
–O_4	2.09	O_4–OH(1)	3.10
–OH(2)	2.03	O_5–O_6	3.14
–O_5	2.08	–OH(2)	3.09
–O_6	2.15	O_6–OH(2)	3.11
mean	2.08	mean	3.11
Angles about T(1)		Angles about T(2)	
O_{11}–T(1)–O_3	117.2°	O_8–T(2)–O_4	110.0°
O_{11}–T(1)–O_7	110.7	O_8–T(2)–O_{11}	111.4
O_{11}–T(1)–O_8	106.1	O_8–T(2)–O_7	105.1
O_3–T(1)–O_7	107.9	O_4–T(2)–O_{11}	112.6
O_3–T(1)–O_8	109.0	O_4–T(2)–O_7	112.2
O_7–T(1)–O_8	105.4	O_{11}–T(2)–O_7	105.3
mean	109.4	mean	109.4
Angles about T(3)		Angles about T(4)	
O_{10}–T(3)–O_{12}	109.1°	O_9–T(4)–O_{10}	111.6°
O_{10}–T(3)–O_9	110.3	O_9–T(4)–O_6	111.9
O_{10}–T(3)–O_5	108.8	O_9–T(4)–O_{12}	108.9
O_{12}–T(3)–O_9	106.7	O_{10}–T(4)–O_6	113.2
O_{12}–T(3)–O_5	109.0	O_{10}–T(4)–O_{12}	106.0
O_9–T(3)–O_5	112.9	O_6–T(4)–O_{12}	104.8
mean	109.5	mean	109.4

* Apical oxygens.
Standard deviation for all bond lengths is 0.02 Å.

liable water content was difficult to obtain but the sample was found to lose ~4% of its weight at 120°C. On this basis, about one water molecule may be associated with each formula unit.

Interlayer water molecules

If vermiculites having two sheets of water molecules between their silicate layers are dehydrated, a phase is produced in which single sheets of water molecules are interleaved with the silicate layers (de la Calle *et al.*, 1985). Vermiculites having single interlayer water sheets contain extensive stacking disorder which causes their $0kl$ reflections, where $k \neq 3n$, to be streaked. As a result of their degraded diffraction patterns, the hydrates with single water sheets are not structurally well defined.

This study has shown that the water molecules in the vermiculite-anilinium intercalate are also in a planar network, albeit a slightly puckered network. Although the positions of the water molecules have not been uniquely determined, the comparatively sharp sub-cell reflections used for the work have allowed their probable positions in an average sub-cell to be found. Earlier studies have only been able to determine x and z coordinates from $h0l$ reflections (de la Calle *et al.*, 1985).

The x and y coordinates for the water molecules in the intercalate are essentially the same as those for water molecules forming the upper and lower triangular faces of the octahedrally arranged clusters about cations in vermiculites having two interlayer water sheets. On dehydration, a phase having a single water sheet forms from a phase having two water sheets if three out of every six water molecules are lost. This process can be thought of as a movement of either an upper or lower triad of water molecules from an octahedron to the middle of the interlayer. Apparently the cations may also be partially displaced from their positions at the middle of the interlayer.

Structure of the silicate layers

The structure of a natural two-layer Mg-vermiculite from Llano, Texas, was determined and comprehensively described by Shirozu and Bailey (1966). The material was found to be affected by stacking disorder, as was the Kenya vermiculite studied earlier by Mathieson and Walker (1954). Because the anilinium intercalation reaction substantially reduces the stacking disorder of vermiculites and thereby reduces streaking in their XRD patterns, these are measured more easily. The details of the silicate part of the intercalated structure, although partially damaged by acid attack, are of interest if determined from such an "improved" diffraction pattern.

Table 5 gives the structural data for Llano vermiculite as calculated from the positional coordinates in Table 3. Except for the averages of the bond lengths about individual tetrahedra, the data in Table 5 accord well with those given for Llano vermiculite by Shirozu

https://doi.org/10.1346/CCMN.1987.0350303 Published online by Cambridge University Press

and Bailey (1966). The present averages for the tetrahedral bond lengths do not show the consistent differences necessary to confirm the *long-range* Si/Al ordering pattern described by Shirozu and Bailey (1966). The errors associated with the T–O bonds in the intercalate are greater than those claimed by Shirozu and Bailey (1966) and may obscure any differences associated with *long-range* ordering. That *short-range* Si/Al ordering occurs in Llano vermiculite is shown by the nuclear magnetic resonance ^{29}Si spectrum of Thompson (1984). This spectrum showed three peaks; hence, over short distances at least, three non-equivalent sites must exist for Si atoms. For these three sites to exist in an ordered array through the crystal, the symmetry must be lower than *C*2/*c* as used by Shirozu and Bailey (1966).

The average T–O bond length determined by this study for all tetrahedral sites is 1.65 Å; therefore, from the regression equation given by Hazen and Burnham (1973) it is equivalent to a composition of $Si_{2.92}Al_{1.08}$ over all tetrahedral sites. Table 2 shows that from the microprobe analyses, this value is $Si_{2.91}Al_{1.04}$.

ACKNOWLEDGMENTS

We thank P. A. Stone for assistance with data collection and processing and E. Horn for assistance in determining the unit-cell parameters.

REFERENCES

Brown, C. J. (1949) The crystal structure of aniline hydrochloride: *Acta Crystallogr.* **2,** 228–232.

Busing, W. R., Martin, K. O., and Levy, H. A. (1962) ORFLS, a Fortran crystallographic least-squares program: *Oak Ridge Natl. Lab. Tech. Mem.* **305,** Oak Ridge National Laboratory, Tennessee, 75 pp.

de la Calle, C., Suquet, H., and Pezerat, H. (1985) Vermiculites hydratées à une couche: *Clay Miner.* **20,** 221–230.

Guss, J. M., Nockolds, C. E., and Wood, A. M. (1970) User manual for a computer-controlled BUERGER-SUPPER equi-inclination X-ray diffractometer: Crystal Structure Laboratory, School of Chemistry, Univ. Sydney, Sydney, Australia, 34–35.

Hazen, R. M. and Burnham, C. W. (1973) The crystal structures of one-layer phlogopite and annite: *Amer. Mineral.* **58,** 889–900.

International Tables for X-ray Crystallography (1974) Vol. IV: Kynoch Press, Birmingham, United Kingdom, 72–78.

Mathieson, A. McL. and Walker, G. F. (1954) Crystal structure of magnesium-vermiculite: *Amer. Mineral.* **39,** 231–255.

Motherwell, W. D. S. (1978) PLUTO78. A plotting program for Cambridge crystallographic data: Chemical Laboratory, Cambridge Univ., Cambridge, United Kingdom, 26 pp.

Nitta, I., Watanabe, T., and Taguchi, I. (1948) The crystal structure of aniline hydrobromide: *X-Sen* **5,** 31–36.

Raupach, M., Slade, P. G., Janik, L., and Radoslovich, E. W. (1975) A polarized infrared and X-ray study of lysine-vermiculite: *Clays & Clay Minerals* **23,** 181–186.

Sheldrick, G. M. (1976) SHELX. Program for crystal structure determination: Cambridge Univ., Cambridge, United Kingdom, 150 pp.

Shirozu, J. and Bailey, S. W. (1966) Crystal structure of a two layer Mg-vermiculite: *Amer. Mineral.* **52,** 1124–1143.

Slade, P. G. and Raupach, M. (1982) Structural model for benzidine-vermiculite: *Clays & Clay Minerals* **30,** 297–305.

Slade, P. G., Raupach, M., and Emerson, W. W. (1978) The ordering of cetylpyridinium bromide on vermiculite: *Clays & Clay Minerals* **26,** 125–134.

Slade, P. G. and Stone, P. A. (1983) Structure of a vermiculite-aniline intercalate: *Clays & Clay Minerals* **31,** 200–206.

Slade, P. G. and Stone, P. A. (1984) Three-dimensional order and the structure of aniline-vermiculite: *Clays & Clay Minerals* **32,** 223–226.

Slade, P. G., Stone, P. A., and Radoslovich, E. W. (1985) Interlayer structures of the two-layer hydrates of Na- and Ca-vermiculites: *Clays & Clay Minerals* **33,** 51–61.

Thompson, J. G. (1984) ^{29}Si and ^{27}Al nuclear magnetic resonance spectroscopy of 2:1 clay minerals: *Clay Miner.* **19,** 229–236.

Tokonami, M. (1965) Atomic scattering factor for O^{2-}: *Acta Crystallogr.* **19,** p. 486.

Ware, N. G. (1981) Computer programs and calibration with the PIBS technique for quantitative electron probe analysis using a lithium-drifted silicon detector: *Computers and Geosciences* **7,** 167–184.

(Received 21 April 1986; accepted 22 November 1986; Ms. 1582)

https://doi.org/10.1346/CCMN.1987.0350303 Published online by Cambridge University Press